Ultramicroscopy 16 (1985) 101–114
North-Holland, Amsterdam



# DIRECT ATOMIC IMAGING OF SOLID SURFACES
## III. Small particles and extended Au surfaces

David J. SMITH *

*High Resolution Electron Microscope, Department of Metallurgy and Materials Science, University of Cambridge, Free School Lane, Cambridge CB2 3RQ, UK*

and

L.D. MARKS **

*Cavendish Laboratory, University of Cambridge, Madingley Road, Cambridge CB3 0HE, UK*

Received 8 August 1984

Atomic-resolution micrographs of small metal particles and extended gold surfaces are presented which demonstrate that detailed surface morphology, including mono-atomic steps and facetting, can be imaged directly in profile. Recent results are briefly reviewed, and further observations are described which concentrate upon dynamic changes in the surface structure. Following electron-beam-induced etching of the carbonaceous surface layer in the presence of water vapour, considerable macroscopic and microscopic rearrangements of the extended films, including surface diffusion, occur. Images recorded in a [0$\bar{1}$1] projection indicate that the (111) surface expands outwards, developing a hill-and-valley morphology, and surface dislocations are seen. The (110) and (100) surfaces were generally microscopically rough with surface partial dislocations again visible on the latter. The presence of surface steps, particularly on (100), was found to have a marked effect on the overall direction of surface diffusion.

## 1. Introduction

A variety of bulk diffraction techniques are available for the characterisation of surfaces, their crystallography and chemical reactions, and the invaluable information which these methods can provide, for example, about surface phenomena such as ordered overlayers, relaxations and surface reconstructions, has recently been reviewed [1]. Most of these techniques involve averaging over extended areas and cannot therefore provide details of local topography. Such real space information, for example about local surface inhomogeneities, can, however, be directly provided by electron microscopy, and applications have recently led to further advances in knowledge and understanding of surfaces and their morphology. Some of these are mentioned below and reference should also be made to the general reviews by Venables [2] and Howie [3].

Despite typical lateral resolution of only 1 nm or greater, surface steps in projection have been observed in gold [4,5], magnesium oxide [6], silicon [7] and silicon carbide [8] using conventional transmission electron microscopes (CTEM) operated in either bright- or dark-field modes and in magnesium oxide using the scanning TEM [9]. Images of vicinal surfaces of gold and platinum at ~ 0.9 nm resolution have been obtained [10] using reflection (or glancing angle) electron microscopy (REM). Atomic steps on the Si(111) surface and the influence of the steps on nucleation of the

* Now at Centre for Solid State Science and Department of Physics, Arizona State University, Tempe, Arizona 85287, USA.
** Now at Department of Physics, Arizona State University, Tempe, Arizona 85287, USA.

(7 × 7) surface reconstruction have also been observed [11] using REM. More recently, extensive studies have been made [12,13] of reconstructed Ag surfaces prepared in situ and observed under Ultra-High-Vacuum conditions which thereby avoids, as pointed out elsewhere [14], possibly misleading results which could have been caused by poorly prepared and characterised surfaces.

In the conventional TEM mode of operation, atomic-level resolutions have recently become obtainable [15] and it has been demonstrated [16,17], using 500 kV high-resolution electron microscopy (HREM), that considerable direct information on this scale about surfaces of small metal particles in a projection configuration was available. For example, direct atomic imaging of a reconstructed metal surface has been achieved for the first time in a TEM [16] and the so-called missing-row model [18] for the 2 × 1 gold (110) surface has been confirmed. Direct measurement of a 20 ± 5% surface relaxation has also proved possible [19]. Subsequently, elastic distortions and plastic deformations have been observed at extended Au(111) surfaces which result, after surface cleaning, in the development of a pronounced hill-and-valley structure [20,21]. In this paper, we first review our observations of the surfaces of small metal particles. Novel observations are then presented of extended Au(110), (111) and (100) surfaces which, in particular, highlight the markedly different atomic rearrangements which are found to take place once the carbonaceous surface contaminant layer is removed by in situ etching. Finally, we briefly mention the validity and likely applicability of direct atomic imaging of surfaces, both for catalysis studies and for surface science generally.

## 2. Experimental

The small metal particles (of gold and silver) were prepared in a small vacuum chamber by epitaxial growth on substrates of NaCl and KCl which had been cleaved in situ. This was followed by evaporation of a carbon film (of ~ 5–10 nm thickness) with subsequent transfer onto microscope grids using flotation in an ethanol/water mix. However, these particles were not generally appropriate for detailed surface observations since the in situ etching inside the electron microscope (see later) removed the carbon support film. As a better system for examining clean surfaces, semi-continuous poly-crystalline films of gold were prepared (by evaporating more metal) and then annealed for at least 24 h to promote grain growth and remove residual strains, before transferral onto holey carbon support films ready for electron microscopy.

The samples were observed with the Cambridge University High Resolution Electron Microscope [23] operated at either 500 kV or 575 kV. This microscope has an interpretable resolution of better than 0.18 nm [24] with the primary {111} (0.235 nm) and {200} (0.204 nm) diffracted beams transferred by the imaging system with relatively small damping factors. Imaging conditions included a beam convergence semi-angle of ~ 0.3 – 0.5 mrad, a focal spread of ~ 16 nm, and an electron-optical magnification of ~ $8 \times 10^5$. This magnification reduced the deleterious effect of statistical noise in the micrographs, although this remained the major limitation on quantitative image measurements. At best, it was possible to measure surface relaxations with an uncertainty estimated to be ~ 5% [25]. An image pick-up and viewing system attached to the microscope [26] was used for choosing the appropriate defocus (black *or* white contrast at the atom positions), and for correction of beam tilt and objective lens astigmatism. A small air-leak valve was introduced into the vacuum system to facilitate etching by water vapour of carbonaceous material initially present on the semi-continuous films. Removal of carbonaceous films is well-known in electron microscopy (see, for example, ref. [27]) *. Image simulations and digital image analysis were used extensively throughout this study, both to establish the appropriate imaging conditions and also to determine how to interpret the images in terms of atomic scale surface features [25]. All the high resolution images presented here were recorded with the samples aligned on the [1$\bar{1}$0] zone axis.

* Observations of carbon film etching in a VG501 STEM, with a mass spectrometer to measure residual gas partial pressures, confirmed that water vapour was the active agent, rather than oxygen.

## 3. Small metal particles

Our initial high resolution observations of small metal particles involved the use of lattice imaging methods, and these studies enabled the characterisation of typical particle morphologies [28,29] to be made and the presence of dislocations in icosahedral multiply-twinned particles (MTPs) to be unequivocably established [30]. However, it was only during a later detailed study of the defects occurring in these MTPs [31], when the interpretable resolution of the microscope was improved from about 0.22 nm to around 0.18 nm, that the possibilities for direct atomic imaging of the surface structure of these particles first became evident.

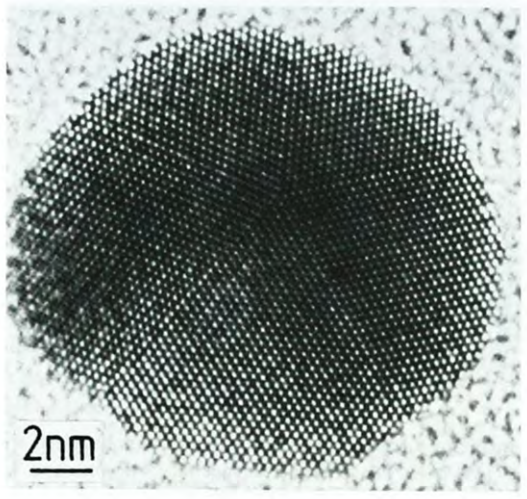


Fig. 1. High-resolution electron micrograph of a decahedral MTP of gold supported on amorphous carbon, prepared by evaporation at room temperature onto KCl in UHV. The pronounced facetting should be noted.

The edge appearance of these small particles is illustrated by those shown in figs. 1 and 2. The image of fig. 1 was recorded at the "reverse contrast" position at 500 kV, where the atomic column positions appear white, and shows a decahedral MTP of gold which, to first order, consists of five twinned tetrahedra. This particle exhibits pronounced micro-facetting in each tetrahedral unit with {111}- and {100}-type facets clearly predominating. This morphology correlates well with the somewhat rounded equilibrium shape of these particles [22]. Fig. 2 shows images of two icosahedral particles of silver, recorded at 575 kV at the optimum defocus condition, and the atomic columns appear black. The surface morphology of these particles is clearly apparent with relatively flat (111) faces and a little additional {110} facetting. Note the microtwin (T) visible in fig. 2a, and

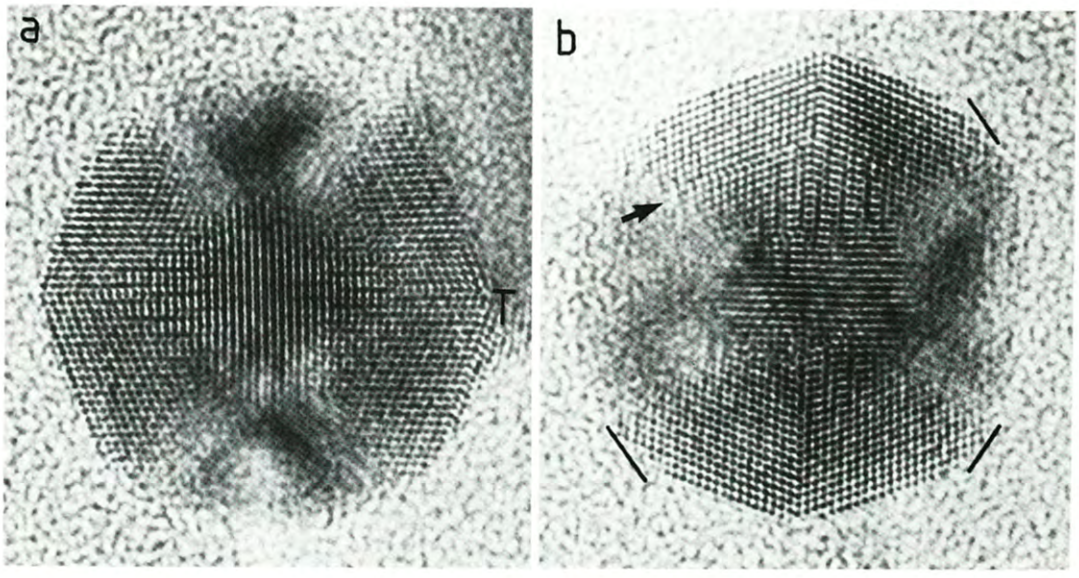


Fig. 2. Micrographs of two icosahedral particles of silver prepared by evaporation in a diffusion-pumped system onto NaCl at 300°C. In both cases the atomic columns are black. Areas of minor {110} facetting are marked. Note twin (T) and stacking fault arrowed.

the small stacking fault arrowed in fig. 2(b).

Although multiply-twinned particles are of intrinsic interest in view of their high internal strain ($\sim$ 2–6% – see, for example, ref. [32]), as well as the existence of dislocations primarily within the icosahedral particles, these same features make them far from ideal for interpreting image features in the vicinity of their surfaces. Therefore, it was decided to investigate small (100) epitaxial square-pyramid nuclei prepared on KCl in the presence of $10^{-6}$ Torr residual impurities, primarily water vapour (i.e. an unbaked UHV system). As shown by the weak-beam image of fig. 3, these particles possessed extensive, flat (111) facets two of which are parallel with the incident electron beam direction when the specimen is tilted by 45° to a (110) pole. An example of a particle in this surface profile imaging mode is shown in fig. 4. Detailed image simulations, using the fact that the particle morphology permitted unambiguous thickness measurements, confirmed that the micrographs recorded were valid images of the atomic surface structure [25].

Under normal circumstances the particles were covered by the carbonaceous support film, and there was no evidence for any surface expansions or reconstructions, i.e. the edge termination appeared to maintain the bulk lattice structure and composition, although there were some indications of small surface contractions of perhaps 1–2%, too small with respect to the error bars of the measurement of $\pm 5\%$ to be significant. However, under etching conditions due to water vapour from photographic negatives or from a deliberate air leak, the carbon coating was gradually removed and some re-ordering of the metal surface took place. For example, as shown in fig. 5, the {110} gold surface of a square pyramidal particle was observed to reconstruct partially to a $2 \times 1$ surface (i.e. having a double period along a ⟨100⟩ direction). The appearance of this image agreed with that expected of the proposed missing-row model for this surface [18] and this agreement was subsequently confirmed by detailed image simulations [16,19]. Further experimental evidence for this model has recently been independently obtained by X-ray diffraction [33] and scanning tunneling microscopy [34]. Careful measurement of this image indicates that the outermost column of gold atoms are relaxed outwards by about $20 \pm 5\%$ [19]

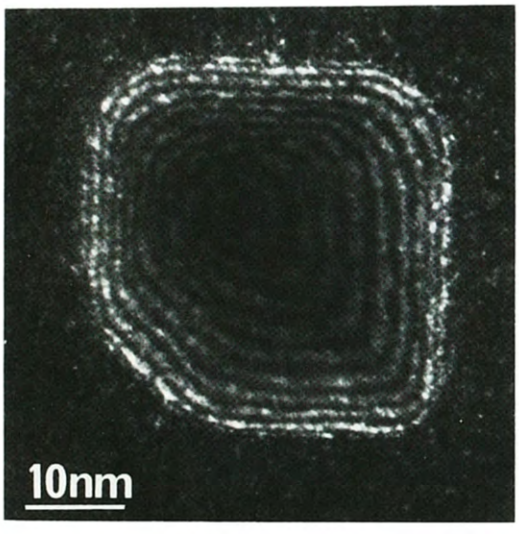


Fig. 3. Weak beak dark field image of a square pyramidal particle of gold which, atypically, has one additional (110) facet.

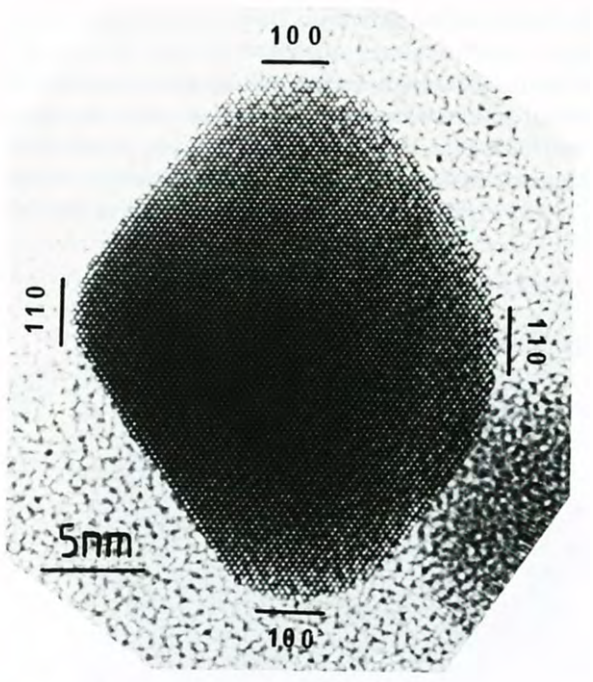


Fig. 4. Image of a square pyramidal particle of gold, tilted by 45° to a $(1\bar{1}0)$ pole. The different surface facets are marked.

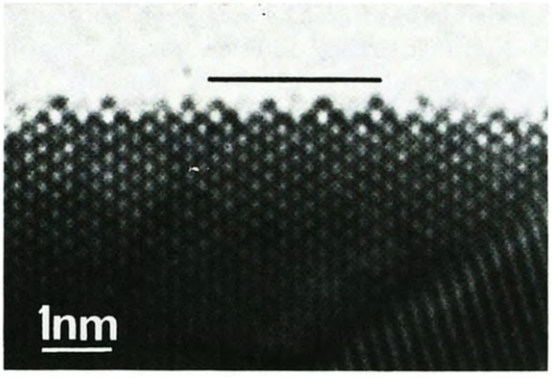


Fig. 5. Area of gold (110) surface which has partially reconstructed to a 2×1 surface mesh.

which is consistent with the 40 ± 30% expansion measured by X-ray diffraction [33]. Note that more recent X-ray and ion scattering experiments [35,36] have unambiguously confirmed the presence of a large expansion and this is probably the only current example of an independent confirmation of a localised HREM result.

## 4. Extended Au surfaces

In our observations of the extended Au surfaces, it was first necessary to remove the overlying carbonaceous layer in order to produce clean surfaces – the change to the surface morphology was otherwise imperceptible. The removal was effected using residual water vapour [27] under the catalytic influence of the incident electron beam (probably similar to the water–gas reaction). This removal process normally took about 30 min although it was found that persistent, partially ordered, monolayers often remained for some period thereafter (perhaps a further 30 min). Moreover, removal meant that the image granularity resulting from surface overlayers no longer interfered with the image originating from Au, thereby resulting in a substantial improvement in the image contrast.

### *4.1. (110) Surface*

Since this particular surface of the small and clean gold particles displayed the 2 × 1 reconstructed superstructure once the carbon layer had been etched away, our initial purpose was to discover whether the same superstructure would develop on the extended surfaces. Unfortunately, substantial surface diffusion continued throughout observation, perhaps because the surfaces were not truly crystallographically flat, and the (110)

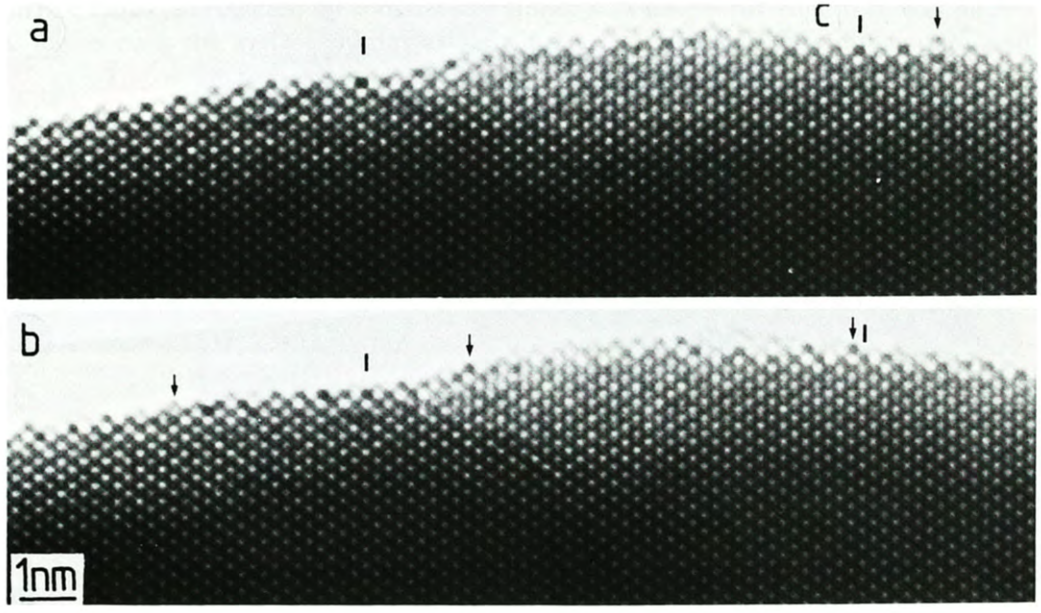


Fig. 6. Two successive exposures showing an area of extended Au(110) surface from the polycrystalline specimen, after most of the initial carbon coverage has been removed. Note movement of gold atomic columns (arrowed).

surfaces tended to re-facet or roughen.

The surface re-ordering is clearly visible, for example, in fig. 6 which shows two consecutive images of the same surface area, both recorded at the same "black atom" focus. The fiducial marks provided enable the appearances of particular local areas to be compared. Note the general irregularity of the surface, in particular the features arrowed which are *columns* of gold atoms which have completely moved between the two exposures (of $\sim 4\frac{1}{2}$ s duration and $\sim 15$ s apart). It should be noted that the sideways shift of atomic columns was only to sites *in-register* with the bulk lattice. In the area marked C there also appears to be some residual carbonaceous material. There are significant differences in the intensities of the outermost columns of atoms which could be due both to a different number of Au atoms in the columns, as well as to the movement of atoms during the period of exposure. Such rapid changes of intensity of appearance were often observed in real time using the image pick-up and viewing system attached to the microscope. However, it has not yet been clearly established whether this site "hopping" was always entirely random. There was some circumstantial evidence, by comparing successive exposures, that surface diffusion was resulting in the development of microfacets. Similarly, the migration of an ordered column of atoms is not unreasonable; migration of part of a column would introduce a high energy surface kink which, being highly mobile, would rapidly diffuse out to leave a perfect column.

A further pair of images of the same surface region, recorded some ten minutes later, are shown in figs. 7a and 7b. Comparison with figs. 6a and 6b indicates that there is no marked change in the overall surface contours (although, as will be shown later, this was not found to be true of the (111) surfaces). However, careful comparison establishes that considerable changes in the local surface features has again occurred, even between these latter two exposures. Indeed, at the point arrowed, it appears that one whole column of atoms has moved sideways to the adjacent site(s). It was also observed, as in fig. 8a, that particular regions sometimes developed 331 microfacets, and fig. 8b shows restricted areas which had either the normal $1 \times 1$ surface structure or the $2 \times 1$ superstructure. Note also that the outermost atomic columns in many

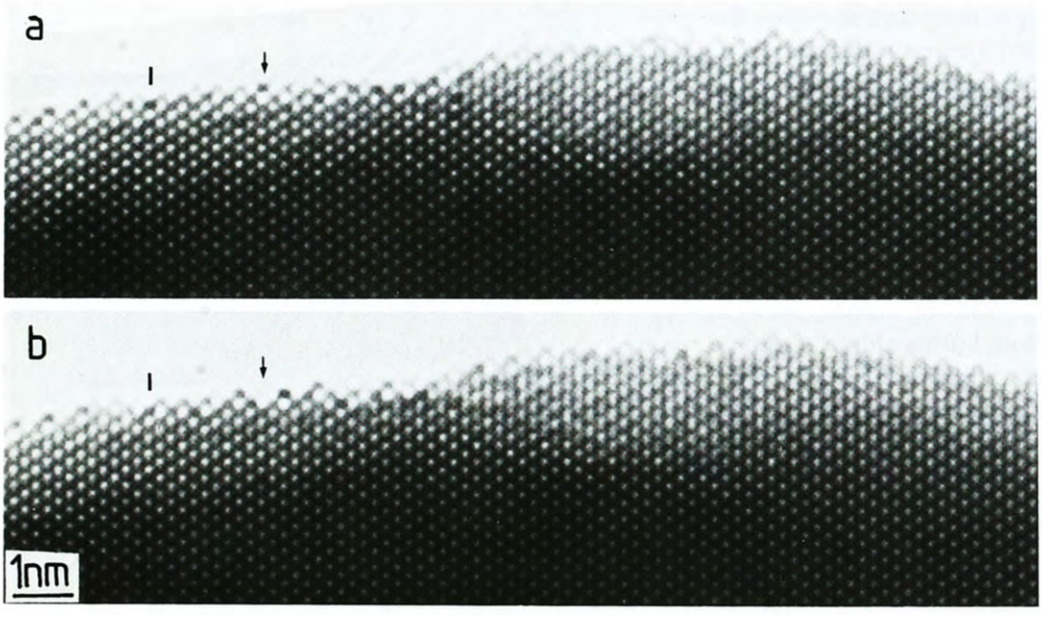


Fig. 7. Two successive exposures of the area shown in fig. 6, recorded some ten minutes later. Note the sideways shift of the atomic column arrowed.

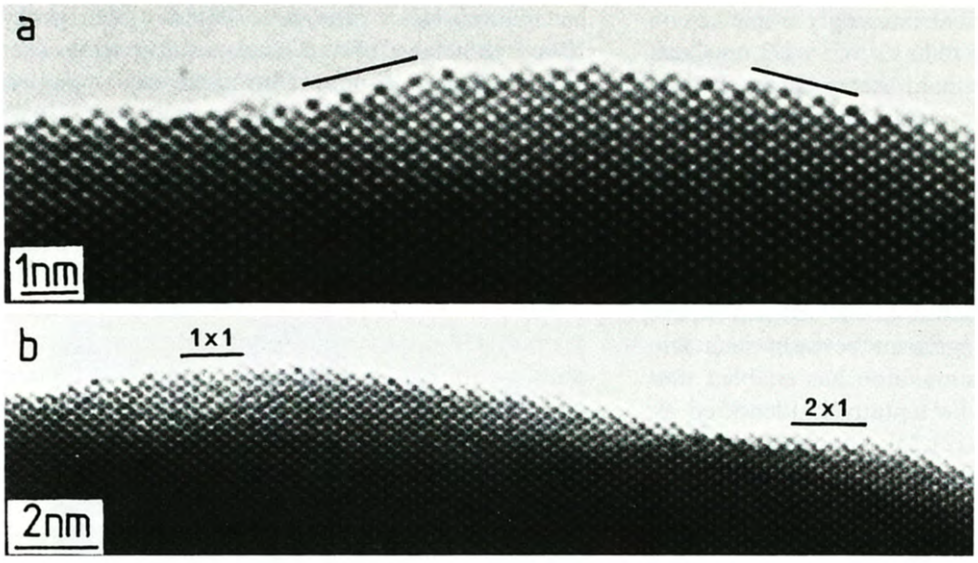


Fig. 8. (a) Area of Au(110) surface showing development of microfacetting. (b) Area of Au(110) surface showing small regions of $1\times1$ and $2\times1$ surface structure.

places are considerably displaced (i.e. relaxed) away from the bulk metal.

*4.2. (111) Surface*

In similar fashion to the (110) surface, the (111) surface displayed evidence for considerable atomic diffusion once the surface overlayers were fully removed. However, as noted earlier, an ordered monolayer was frequently found to remain long after most of the overlayer disappeared. A useful criterion for identifying the presence of this surface overlayer proved to be the change of the local image appearance which occurred as the objective lens focus condition was altered [25], since this was found to be different for gold and carbon. For

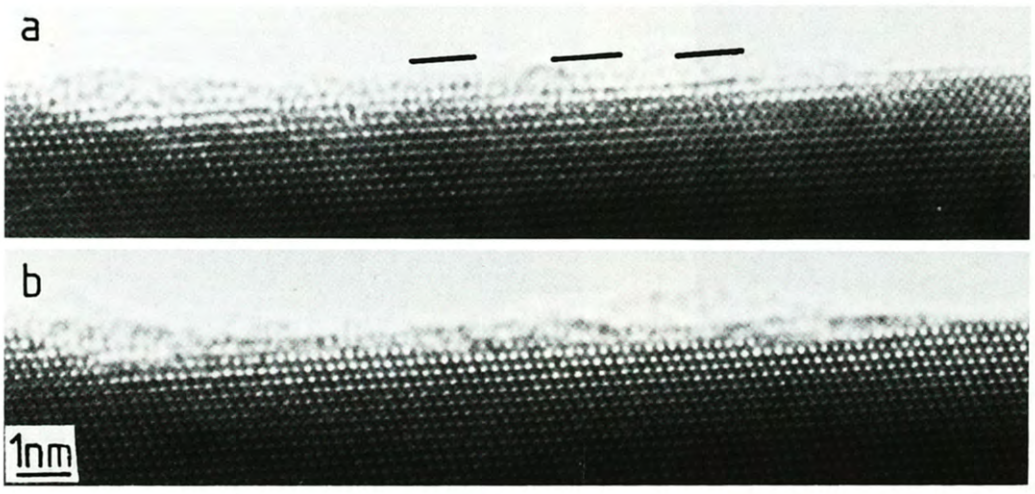


Fig. 9. A defocus pair of images of the (111) surface (a) optimum defocus (black Au atomic columns). (b) reverse contrast (white Au atoms columns). Ordered carbonaceous surface layer marked.

example, with the typical imaging parameters of the present microscope (500 kV, $C_s = 2.7$ nm), the contrast of columns of gold atoms changed from back to white on going from a defocus of $-67.5$ nm to $-97.5$ nm, whereas columns of carbon atoms, in most cases, appeared black at $-67.5$ nm, but had very weak contrast at $-97.5$ nm. This effect can be clearly seen in experimental images such as the focus pair in fig. 9 – the areas marked here show the characteristics of the ordered superstructure. Careful comparisons between such micrographs and image simulation has enabled this ordered monolayer to be tentatively identified as consisting of benzene [21,25]. In order to avoid any confusion over image interpretation and possible artefacts, it was common during the present study to record images at both the "black dot" and "white dot" focus positions. (Note, however, that these pairs are not always shown here.)

The macroscopic structural changes observed in images of the (111) surfaces have been described elsewhere [20,21] and can be understood in terms of a positive tangential surface pressure on the clean gold surface. Removal of the carbon overlayers led initially to the development of an irregular hill-and-valley structure, typically with peak-to-trough heights of 5–6 interatomic spacings (i.e. ~ 1.0–1.2 nm), as shown in fig. 10, accompanied by spatially varying normal relaxations (~ 5–10%) of the first atomic layer interplanar spacing. At a later stage, the extent of surface normal relaxation generally decreased but stress-relieving surface dislocations were then often observed to develop (see

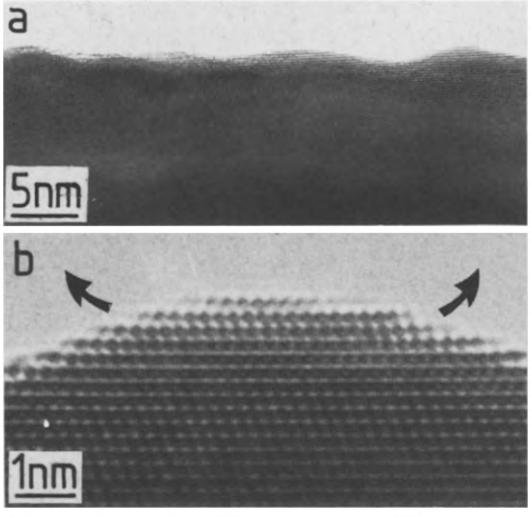


Fig. 10. (a) Low magnification image of (111) surface showing development of hill-and-valley structure after removal of carbon. (b) High magnification image showing comparatively well-ordered (111) surface with some small expansions (indicated).

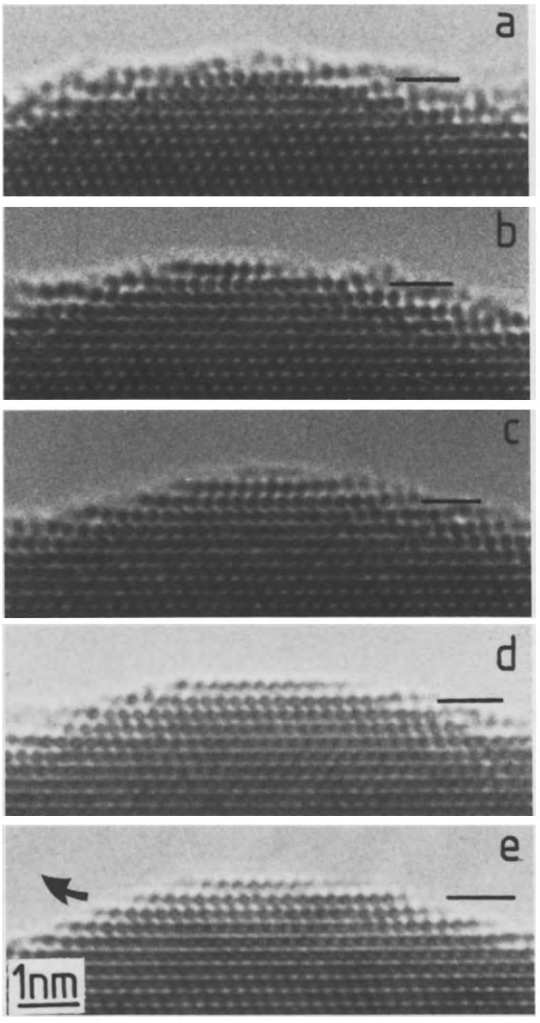


Fig. 11. Series of images, recorded over a 20 min period, showing several stages in "hill" development. In (a) some carbon remained, but in (b) a new twinned surface layer has grown, which extended in length in (c). In (d) this stacking fault has gone whilst, in (e), this layer has been shortened and the overall feature is now well-ordered. Marker indicates original surface layer.

below). Note that the concept of such lattice distortions and dislocations is entirely consistent with models of pseudomorphic growth (see, for example, [37,38]).

Some interesting effects were again observed during the atomic rearrangements which took place on this surface. The series of images shown in figs. 11a–11e records the evolution, over a time period of about 20 min, of a further surface layer which gradually accumulates on top of one of the "hills". Fig. 11a shows this peak at the time when the last remnants of carbon are being etched away. Note the reference line which is used to depict the position of the initial surface layer throughout the series. In fig. 11b, an extra surface layer of atomic columns, about 6 atom widths long, is now visible in a twinning relationship with the layer beneath it, and in fig. 11c this extra twinned layer is about 10–12 atom widths long, with some suggestion of yet another layer being added above it. In fig. 11d, this layer is no longer twinned with the plane of atoms beneath it, presumably as a result of the passage of a dislocation. Finally, fig. 11e shows this layer, now shortened in length, with the surface relaxations (arrowed) readily apparent. The three images in figs. 12a–12c show another region with a surface stacking fault which, over the passage of time, accumulates above it a further surface layer which includes what can be identified from the atomic column stacking as a surface dislocation. Eventually, as in fig. 12c, this surface layer is rearranged and the layer stacking (of the first four layers) becomes the hexagonal ABAB configuration.

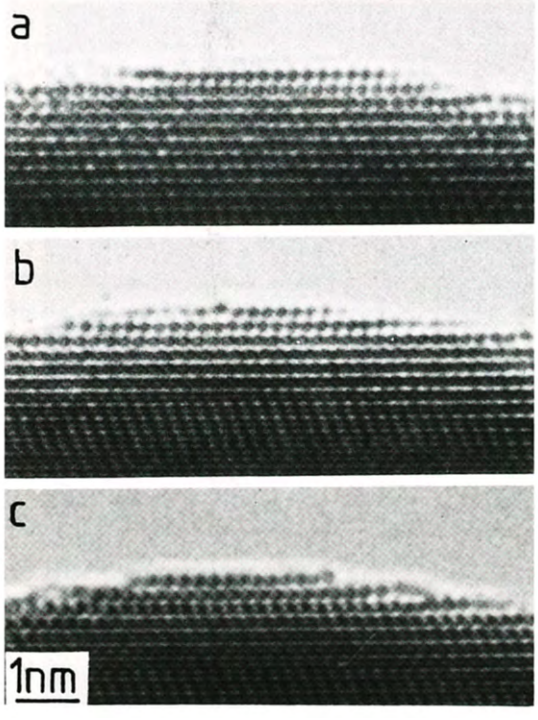


Fig. 12. (a) Surface stacking fault on (111) surface. (b) Same area with a surface partial dislocation now present. (c) Surface layer rearranged to give hexagonal ABAB column stacking.

### 4.3. (100) Surface

Unlike the (110) and (111) surfaces, the (100) surface did not undergo any macroscopic changes when it was reasonably flat and crystallographic, even though considerable diffusion was apparent, as evidenced both by direct viewing and by photographic recording. However, it was significant, as demonstrated below, that mass transfer was observed to be comparatively rapid in the presence of surface steps or ledges. Under these circumstances, the nett atomic migration was consistently found to be in the direction of the lower side of the step. This is not remarkable considering the geometry and energetics of the situation – a surface step is an assymmetric potential barrier to surface diffusion. Finally, it should be recorded that the (100) surface generally appeared to be locally inhomogeneous – both contractions and expansions, typically $\lesssim 10\%$, were visible.

A representative "black dot"/"white dot" pair of images of the (100) surface is shown in figs. 13a and 13b. In this case, a partial carbon overlayer still remains and it appears, as already shown for the (111) surface [21,25], that the surface carbon can be distinguished from the bulk Au by different changes in contrast as the focus is altered. With the passage of time, the carbon continued to be etched away and re-arrangement of the surface occurred. Figs. 14a–14c, for example, show the gradual disappearance, over a period of about 30 min, of the surface shown in fig. 13a. The inclined grain boundary located at the extreme right of each of these images represents a convenient reference line for comparison purposes, and makes it

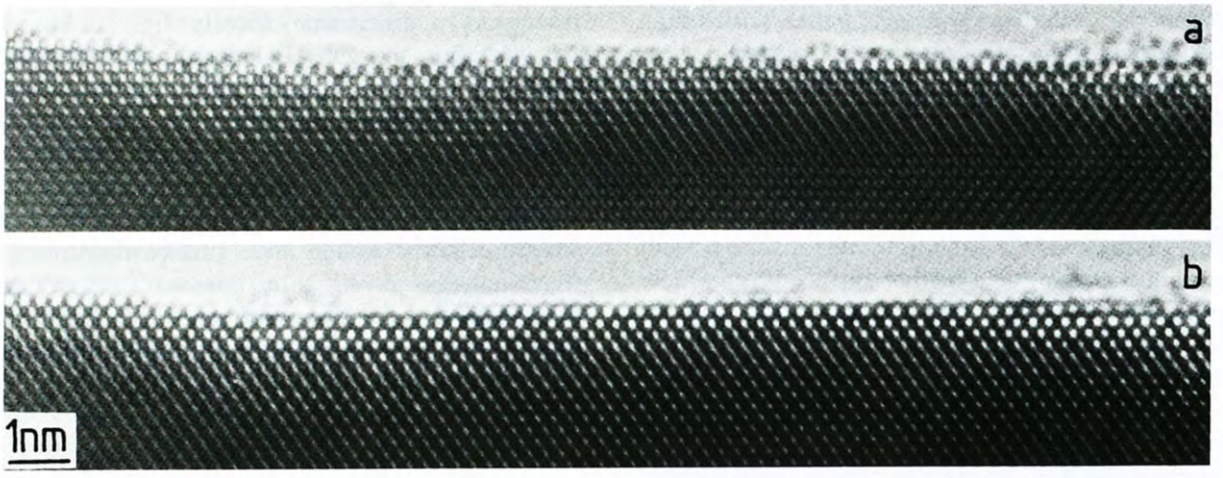


Fig. 13. A defocus pair of images of the (100) surface (a) optimum defocus (black atomic columns); (b) reversed contrast (white).

clear that the "flat" region in fig. 14a, which is ca. 20 nm long, is reduced in length to *ca.* 12 nm in fig. 14b, and is effectively non-existent in fig. 14c. Consideration of the macroscopic change in the surface contours effected by this continual atomic diffusion indicates that this behaviour can be interpreted in terms of the preferential migration from upper surface ledges onto lower sides. A

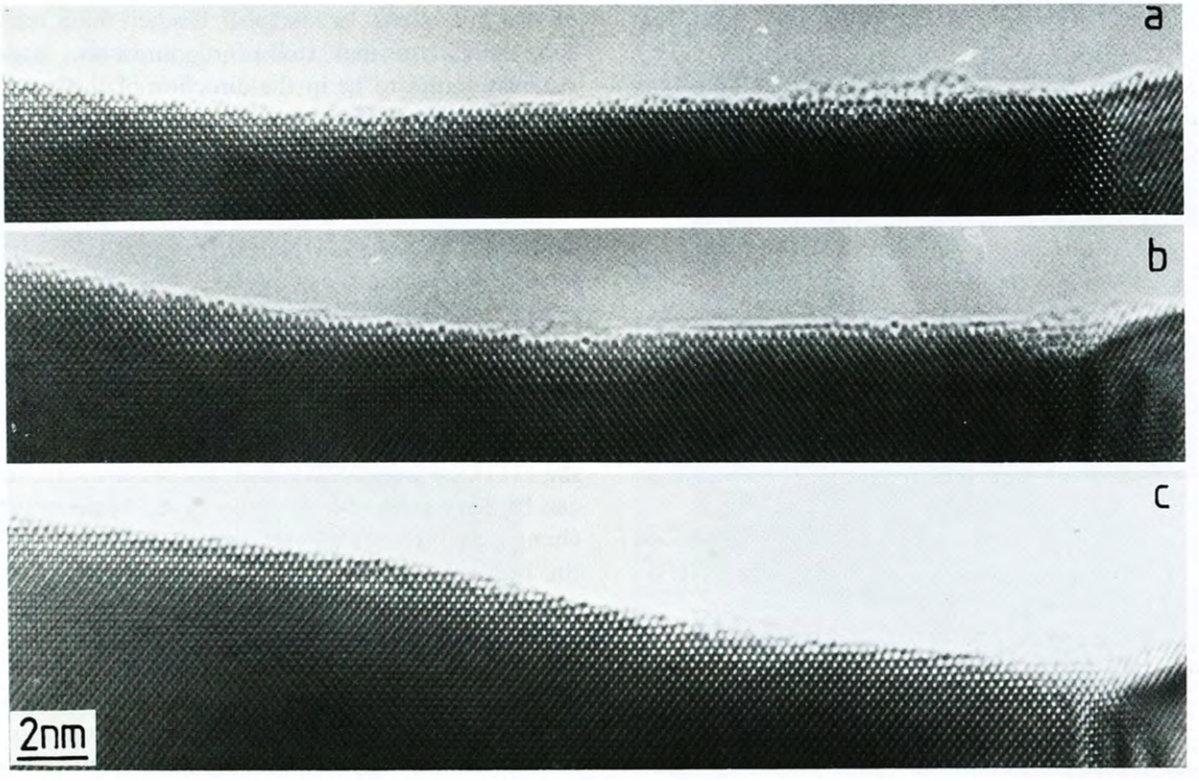


Fig. 14. Series of images of (100) surface recorded over a 30 min period showing substantial alteration of surface contours.

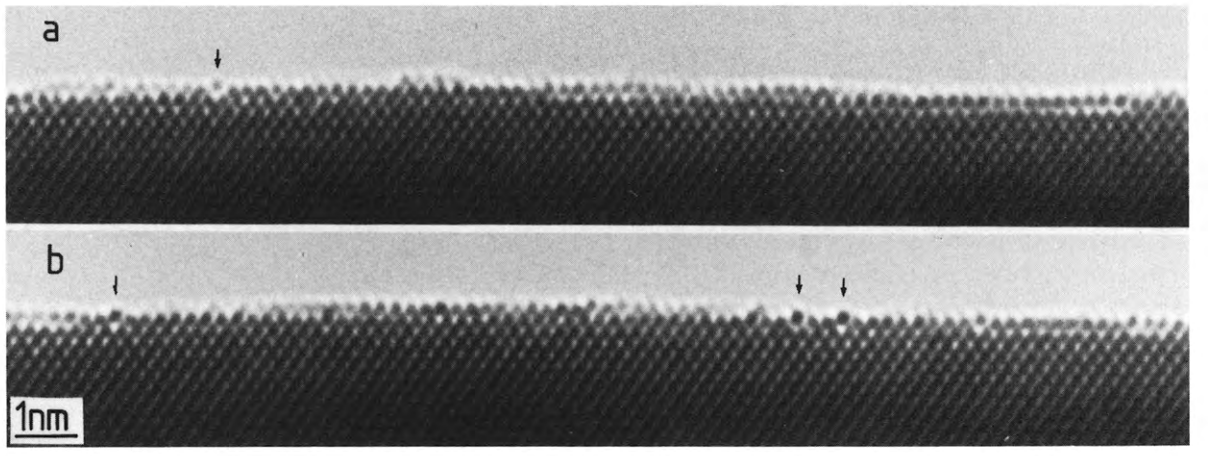


Fig. 15. Successive images of a relatively flat (100) surface showing surface defects, some of which (arrowed) change between exposures.

detailed comparison of atomic rearrangements on different surfaces and further analysis will be given elsewhere [39].

A number of surface defects are visible in figs. 14b and 14c and similar faults are generally found to be a common occurrence on other images of the (100) surface. These defects can best be described as an apparent displacement of an atomic column normal to the surface by $\gtrsim 20\%$ of an interplanar spacing, together sometimes with a slight sideways shift. The pair of images shown in figs. 15a and 15b, which are successive exposures with no change to the imaging conditions, also indicate that these features can, in fact, alter significantly in a comparatively short period of time. As discussed elsewhere [40], these defects are believed to be surface Shockley partial dislocations which provide a mechanism whereby the metastable $1 \times 1$ (100) surface could be transformed to the hexagonal $5 \times 20$ reconstructed surface.

## 5. Discussion

Surface profile imaging, as described above, is unquestionably a highly-promising technique for investigating surface structure at the atomic level. However, given its novelty, it seems appropriate to discuss some aspects of its applicability and validity.

Profile imaging, unlike other normal incidence imaging techniques, is somewhat insensitive to small structural variations along the beam direction, since the final high-resolution image represents a two-dimensional projection of the structure. Details of important surface phenomena, such as kinks at surface steps and inclined reconstructed superstructures, could therefore be difficult to decipher. Conversely, under certain circumstances, the method is sensitive to the presence and nature of any surface overlayer [21,25], so that information about the influence of adsorbates and impurities on surface morphology could be obtainable. However, the realisation of this possibility assumes that the electron beam does not result in any fundamental structural change. Microscopy under the conditions used here (500 kV, electron dose $\gtrsim 10^6\ s^{-1}\ nm^{-2}$) is almost certain to desorb any loosely-attached species, and even the use of low-dose techniques at lower kilovoltages, possibly involving a sensitive image pick-up system, will not always prevent this from happening.

It is clear that the environmental conditions prevailing inside the present HREM do not provide "clean and well-defined surfaces" as can nowadays be obtained with modified [11,14] and custom-built [12,13] instruments. However, gold is a highly inert material which will remain clean even in relatively poor vacuum. Hence, we can be confident that artefacts due to impurities are not

observed, which would not be the case for more reactive materials such as silver. It is worth repeating that, until the carbonaceous surface layer was removed, there was no evidence for any surface re-ordering nor any suggestion of any relaxations. It is therefore possible to conclude that the macroscopic and microscopic rearrangements which have been observed here were not induced by the electron beam but rather occurred as a consequence of the removal of the residual carbon, thereby allowing the various surfaces to reconstruct. Furthermore, the marked difference between the (111) surface (which roughened) and the (100) (which remained flat) is inconsistent with beam damage being the cause of our results. The carbon removal also has the added benefit of enabling better definition to be obtained in the surface profile images since there is no confusing detail then originating from overlapping carbonaceous material.

Finally, it needs to be appreciated that application of the technique to characterisation of small metal particle heterogeneous catalysts will not necessarily be straightforward. Image interpretability effectively relies on a close alignment of a crystallographic zone axis of a particle with the incident beam direction [25]. Location of suitable particles in industrial catalysts could be quite tedious, particularly to satisfy the alignment requirement, and it might prove more profitable to rely on statistical chance and resort to photography of random fields of view. Nevertheless, preliminary images from commerical catalysts have been obtained and these clearly show the atomic surface structure.

## 6. Conclusion

The results presented above demonstrate, unequivocably, that latest developments in HREMs have enabled surface profile imaging on the atomic scale of small metal particles and extended thin films. Local information about surface re-ordering becomes available which compares favourably in surface sensitivity with that provided by bulk diffraction techniques. Moreover, it can also be concluded that unique details of surface morphology, including macroscopic and microscopic rearrangements and information on surface diffusion, can be obtained. Applications of the technique to surface science and catalysis studies, in particular those involving small metal particle heterogeneous catalysts, should result in new and fundamental insights into the properties and behaviour of metal surfaces.

## Acknowledgements

This work has been supported by SERC, UK, and L.D.M. also acknowledges support of Department of Energy (US) Grant No. DE-ACOL-76ER02995.

## References

[1] A.J. Forty, Contemp. Phys. 24 (1983) 271.
[2] J. Venables, Ultramicroscopy 7 (1981) 81.
[3] A. Howie, in: Electron Microscopy and Analysis 1981, Ed. M.J. Goringe (Institute of Physics, London–Bristol, 1982) p. 419.
[4] D. Cherns, Phil. Mag. 30 (1974) 549.
[5] K. Tagi, K. Takayanagi, K. Kobayashi, N. Osakabe, Y. Tanishiro and G. Honjo, Surface Sci. 86 (1979) 174.
[6] K. Kambe and G. Lehmpfuhl, Optik 42 (1975) 187.
[7] S. Iijima, Optik 48 (1977) 193.
[8] S. Iijima, in: Proc. 38th Annual EMSA Meeting, San Francisco, CA, 1980, Ed. G.W. Bailey (Claitor's, Baton Rouge, LA, 1980) p. 376.
[9] J.M. Cowley, in: Proc. 39th Annual EMSA Meeting, Atlanta, GA, 1981, Ed. G.W. Bailey (Claitor's, Baton Rouge, LA, 1981) p. 212.
[10] Tung Hsu, Ultramicroscopy 1 (1983) 167.
[11] N. Osakabe, Y. Tanishiro, K. Yagi and G. Honjo, Surface Sci. 97 (1980) 393.
[12] K. Takayanagi, K. Kobayashi, Y. Kodaira, Y. Yokoyama and K. Yagi, in: Proc. 7th Intern. Conf. on High Voltage Electron Microscopy, Eds. R.M. Fisher, R. Gronsky and K.H. Westmacott (Lawrence Berkeley Laboratory, Berkeley, 1983) p. 47.
[13] K. Takayanagi, J. Microscopy (1984) in press.
[14] K. Yagi, K. Takayanagi and G. Honjo, in: Crystals, Growth, Properties and Applications, Vol. 6 (Springer, Berlin, 1982) p. 48.
[15] D.J. Smith, Helv. Phys. Acta 56 (1983) 464.
[16] L.D. Marks and D.J. Smith, Nature 303 (1983) 316.
[17] D.J. Smith and L.D. Marks, in: Proc. 7th Intern. Conf. on High Voltage Electron Microscopy, Eds. R.M. Fisher, R. Gronsky and K.H. Westmacott (Lawrence Berkeley Laboratory, Berkeley, 1983) p. 53.
[18] See C.-M. Chan, K.L. Luke, M.A. Van Hove, W.H. Weinberg and E.D. Williams, J. Vacuum Sci. Technol. 16 (1979) 642.

[19] L.D. Marks, Phys. Rev. Letters 51 (1983) 1000.
[20] L.D. Marks, V. Heine and D.J. Smith, Phys. Rev. Letters 52 (1984) 656.
[21] L.D. Marks and D.J. Smith, Surface Sci. 143 (1984) 495.
[22] L.D. Marks, Phil. Mag. A49 (1984) 81.
[23] D.J. Smith, R.A. Camps, V.E. Cosslett, L.A. Freeman, W.O. Saxton, W.C. Nixon, H. Ahmed, C.J.D. Catto, J.R.A. Cleaver, K.C.A. Smith and A.E. Timbs, Ultramicroscopy 9 (1982) 203.
[24] D.J. Smith, R.A. Camps, L.A. Freeman, R. Hill, W.C. Nixon and K.C.A. Smith, J. Microscopy 130 (1983) 127.
[25] L.D. Marks, Surface Sci. 139 (1984) 281.
[26] C.J.D. Catto, K.C.A. Smith, W.C. Nixon, S.J. Erasmus and D.J. Smith, in: Electron Microscopy and Analysis 1981, Ed. M.J. Goringe (Institute of Physics, London–Bristol, 1982) p. 123.
[27] H.G. Heide, in: Proc. 5th Intern. Conf. on Electron Microscopy, Ed. S.S. Breese, Jr. (Academic Press, New York, 1962) Vol. 1, p. A4.
[28] L.D. Marks and D.J. Smith, J. Crystal Growth 54 (1981) 425.
[29] D.J. Smith and L.D. Marks, J. Crystal Growth 54 (1981) 433.
[30] D.J. Smith and L.D. Marks, Phil. Mag. A44 (1981) 735.
[31] L.D. Marks and D.J. Smith, J. Microscopy 130 (1983) 249.
[32] A. Howie and L.D. Marks, Phil. Mag. A49 (1984) 95.
[33] I.K. Robinson, Phys. Rev. Letters 50 (1983) 1145.
[34] G. Binnig, H. Rohrer, Ch. Gerber and E. Weibel, Surface Sci. 131 (1981) L379.
[35] I.K. Robinson, Y. Kuk and L.C. Feldman, Phys. Rev. B29 (1984) 4762.
[36] R.J. Culbertson, private communication.
[37] J.H. van der Merwe and C.A.B. Ball, in: Epitaxial Growth, Ed. J.W. Matthews (Academic Press, New York, 1975) p. 493.
[38] J.A. Snyman and H.C. Snyman, Surface Sci. 105 (1981) 357.
[39] D.J. Smith and L.D. Marks, Mater. Res. Symp., in press.
[40] L.D. Marks and D.J. Smith, Surface Sci., submitted.